Voltage Stability Analysis of Grid-Connected Wind Farms with FACTS: Static and Dynamic Analysis

Kevin Zibran Heetun,[a] Shady H.E. Abdel Aleem,[*b] Ahmed F. Zobaa[c]

[a]*College of Engineering, Design & Physical Sciences, Brunel University London, Uxbridge, Middlesex, United Kingdom. E-mail address:* kevin.heetun@theiet.org
[b]*Mathematical, Physical & Life Sciences, 15th of May Higher Institute of Engineering, 15th of May City, Helwan, Cairo, 11731, Egypt. E-mail address:* engyshady@ieee.org
[c]*College of Engineering, Design & Physical Sciences, Brunel University London, Uxbridge, Middlesex, UB8 3PH, United Kingdom. E-mail address:* azobaa@ieee.org
[*]*Corresponding author. T: +201227567489 | F: +2025519101| E-mail address:* engyshady@ieee.org

Abstract- Recently, analysis of some major blackouts and failures of power system shows that voltage instability problem has been one of the main reasons of these disturbances and networks collapse. In this paper, a systematic approach to voltage stability analysis using various techniques for the IEEE 14-bus case study, is presented. Static analysis is used to analyze the voltage stability of the system under study, whilst the dynamic analysis is used to evaluate the performance of compensators. The static techniques used are Power Flow, V–P curve analysis, and Q–V modal analysis. In this study, Flexible Alternating Current Transmission system (FACTS) devices- namely, Static Synchronous Compensators (STATCOMs) and Static Var Compensators (SVCs) - are used as reactive power compensators, taking into account maintaining the violated voltage magnitudes of the weak buses within the acceptable limits defined in ANSI C84.1. Simulation results validate that both the STATCOMs and the SVCs can be effectively used to enhance the static voltage stability and increasing network loadability margin. Additionally, based on the dynamic analysis results, it has been shown that STATCOMs have superior performance, in dynamic voltage stability enhancement, compared to SVCs.

Keywords: Dynamic analysis, FACTS, optimization, power flow, static analysis, voltage stability.

Nomenclature

B_e	Suceptance of SVC
i_{ds}	Direct axis component of the stator current

i_{qs}	Quadrature axis component of the stator current
i_{dr}	Direct axis component of the rotor current
i_{qr}	Quadrature axis component of the rotor current
J	Jacobian matrix of the system
J_R	Reduced Jacobian matrix of the system
P	Real power
Q	Reactive power
r_s	Stator resistance
r_r	Rotor resistance
s	Slip
V_{ds}	Direct axis component of the stator voltage
V_{qs}	Quadrature axis component of the stator voltage
V_{dr}	Direct axis component of the rotor voltage
V_{qr}	Quadrature axis component of the rotor voltage
ω_m	Synchronous speed
X_s	Stator reactance
X_r	Rotor reactance
X_m	Magnetising reactance
ΔV	Change in the voltage matrix
ΔQ	Change in the reactive power
λ_i	The i*th* eigenvalue of J_R

1. Introduction

The depletion of fossil fuel resources and the growing concern for greenhouse gases are triggering many countries to invest in renewable energy resources such as energy production from wind and solar resources. Both wind and solar resources are free and once they are operating, they have almost no greenhouse gas emission associated with them [1]. However, the rapid growth in using renewable-based generation poses challenges for the system operators. In general, they experience intermittency, variability, partial controllability and location dependency. Some of the challenges introduced in [2] include system security, power quality and system stability. Among power system stability concerns, voltage stability, which is addressed in this paper, is one of the major concerns. Voltage stability of networks is still a major issue with major blackouts recently occurred, such as the massive blackout that took place on July 2012 in India affecting around 670 million people, or the partial blackout that took place on September 2014 in Egypt affecting around 20 million people. Typically, according to [3], voltage stability refers to the capability of power system to sustain constant

voltage at all buses after being subjected to a disturbance from a given initial operating point. Moreover, voltage stability can be classified into two categories, according to the type of disturbance, or according to the time span over which instability may occur. Regarding to the type of disturbance, small–disturbance voltage stability can be seen as the ability of the power system to maintain voltage control after a small disturbance such as a load change, whilst large–disturbance voltage stability can be defined as the ability of the power system to maintain voltage control after a large disturbance such as big generation tripping. Regarding to time, short–term voltage stability considers the dynamics of the fast acting loads, whereas long–term voltage stability takes into consideration slower acting equipment. Generally, closeness to voltage collapse can be used to measure voltage stability of a power system. By definition, a voltage collapse is a sequence of events following voltage instability that leads to a blackout or severe low voltage condition in a network. Voltage collapse can be seen as a static phenomenon which is associated with reactive power imbalance [4]. In other words, transmission lines, transformers and loads are sinks of reactive power. Accordingly, if a sufficient reactive power compensator is not available in the power system, voltage instability may occur. Since voltage stability problem is seen as a static phenomenon, it can be addressed by off-line study through the initial design or during network improvement process. Additionally, issues such as the loadability limit of the network, fault ride through capability, reactive power reserve and time respond of these reserves, are all included in voltage stability studies. Furthermore, many distribution networks still operate in an open ring system. Power is restored during faults by moving open points. Hence, the power system network needs to be stable under these new operating conditions.

At the present time, in order to improve the voltage profile, power electronics based devices called Flexible AC Transmission Systems, or FACTS, are being used. FACTS is a family of power electronics devices that is involved in the control of bulk flow of both active and reactive powers [5]. FACTS devices can provide both series and shunt compensation to improve the system's voltage profile and increase loadability of the transmission systems. FACTS may also address other issues in the future, such as sub-synchronous oscillations or

dynamic voltage control [6]. The most common devices that can provide shunt compensation are the Static Synchronous Compensators (STATCOMs) and the Static Var Compensators (SVCs).

In the literature, fault ride through capability has been checked in [7] using a fixed speed induction generator with STATCOM and SVC. Other works on dynamic analysis can be found in [8]. Induction generators need reactive power to operate, thus, they draw it from the grid unless fitted with local reactive power source. On the other hand, the doubly fed induction generator (DFIG) or the synchronous generator can regulate their own power factor from leading to lagging. Mathematical techniques are available to give an insight of the closeness of a system to voltage collapse. They can be classified either static or dynamic. In [4], static voltage analysis was performed using UWPFLOW for P-V curve analysis in order to identify voltage collapse using the Continuation Power Flow (CPF). STATCOM and SVC have been used to improve voltage stability. Tangent vector analysis was used to allocate compensators to the weakest buses. Related works have been done in [9-13].

This paper demonstrates that a combination of both static and dynamic analyses should be used for voltage stability studies. One of the objectives is to devise a systematic approach for voltage stability analysis, which can be used by engineers during network planning. Specifically, load flow analysis, V – P curves and Q – V modal analysis, are used for the static voltage stability analysis. Dynamic analysis is used to re-evaluate the performance of the STATCOM and SVC during contingencies. Time domain simulation for differential algebraic equations for power systems are solved for the dynamic analysis.

2. Wind Farm Modelling

Basically, a wind turbine (WT) is a device that extracts kinetic energy from the air and feeds it to a generator to generate electricity. The axis of the wind turbine can be either horizontal or vertical. In horizontal axis wind turbines, the blades rotate on an axis that is parallel to the ground, whilst in vertical axis wind turbines, the blades rotate on an axis that is perpendicular to the ground. According to [14], wind turbines can be classified into five types, as follows:

(i) Type 1: fixed speed WT with squirrel cage induction generator directly connected to the grid via a step up transformer, (ii) Type 2: limited variable speed WT with wound rotor induction generator, (iii) Type 3: variable speed WT with partial power electronic conversion and Doubly-Fed Induction Generator (DFIG), (iv) Type 4: variable speed WT with full power electronic conversion with both synchronous or induction generators may be used, and (v) Type 5: variable speed with mechanical torque converter between low speed and high speed shaft and synchronous generator. Ref. [15] demonstrated that the most common types are Type 1, Type 3 and Type 4. Nowadays, DFIG is widely being installed because of the following advantages:

- It can operate at variable wind speeds (±33% around synchronous speed). This allows production of electricity at low wind speeds.
- The cost of the inverter is reduced as it handles around 30 % of the total power.
- It can control the amount of reactive power to be supplied or absorbed from the grid, hence controlling the power factor.
- It is more efficient than conventional induction generators.

Figure (1) shows a schematic diagram of a DFIG equipped WT. The stator is directly connected to the grid. The rotor windings are connected to the grid using a back-to-back voltage source converter (VSC) and via slip rings. The VSC is able to deliver a variable frequency source, while permitting a variable speed rotation. The magnetic field, produced in the rotor windings, rotates due to the rotation of the generator's rotor plus the rotational effects produced by the converter AC current. This gives rise to two possibilities where the rotor's magnetic field rotates opposite and in the same direction as the rotor. Super-synchronous operation occurs when the rotor magnetic field is in the same direction as the generator rotor. Sub-synchronous operation occurs when the rotor magnetic field is in the opposite direction of the generator rotor. The magnitude of the induced stator voltage depends on the magnetic flux density passing through the stator windings. A constant voltage can be

maintained at the stator by applying a voltage to the rotor winding which is proportional to the frequency. This implies maintaining the voltage-frequency (V/f) ratio constant [16].

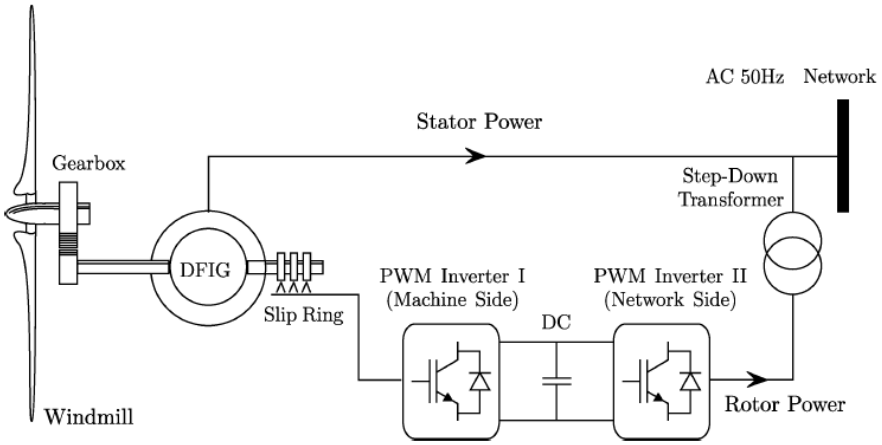

Figure 1. Schematic diagram of a DFIG equipped WT [15]

The steady state model of the DFIG is shown in Figure (2). Subscripts '*d*' and '*q*' refer to the direct and quadrature axis components. The remaining terms in the equations that follow are described in Figure (2) itself, in addition to the Nomenclature. A detailed analysis is provided in [17]. It is assumed that the stator and rotor flux dynamics are much faster compared to the grid dynamics. The converter decoupled the DFIG from the grid. Under these assumptions, the stator circuit is represented by Equations (1) and (2).

$$v_{ds} = -r_s i_{ds} + \left(x_s + x_m\right) i_{qs} + x_m i_{qr} \tag{1}$$

$$v_{qs} = -r_s i_{ds} - \left(x_s + x_m\right) i_{ds} + x_m i_{dr} \tag{2}$$

Additionally, the rotor circuit is described by Equations (3) and (4).

$$v_{dr} = -r_r i_{dr} + \left(1-\omega_m\right)\left(\left(x_r + x_m\right) i_{qr} + x_m i_{qs}\right) \tag{3}$$

$$v_{qr} = -r_r i_{qr} - \left(1-\omega_m\right)\left(\left(x_r + x_m\right) i_{dr} + x_m i_{qs}\right) \tag{4}$$

The per-unit real power (P) injected into the grid, when the losses are ignored, is the sum of the stator and rotor powers as shown in (5).

$$P = v_{ds} i_{ds} + v_{qs} i_{qs} + v_{dr} i_{dr} + v_{qr} i_{qr} \tag{5}$$

Similarly, the per-unit reactive power is given by the sum of the stator reactive power and that of the grid side converter. Equation (6) represents the reactive power that the stator will

either absorb or release to the grid.

$$Q = v_{qs} i_{ds} - v_{ds} i_{qs} \quad (6)$$

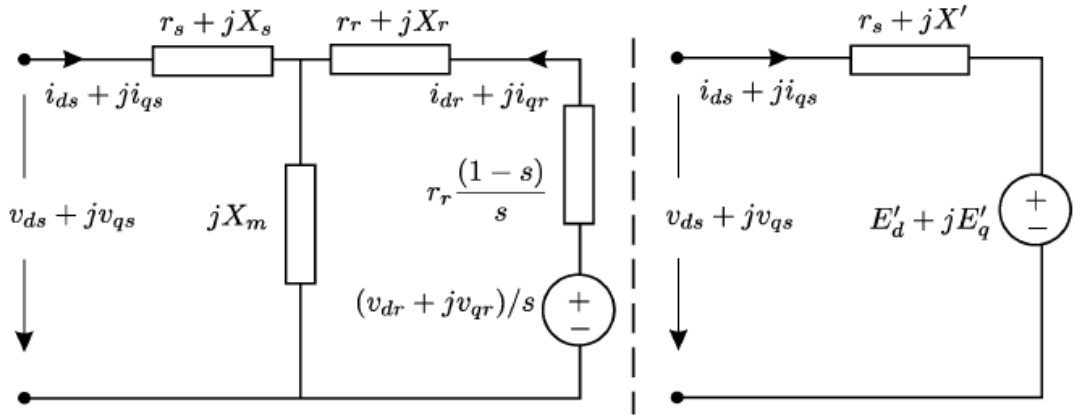

Figure 2. Equivalent circuit (per-phase) of the DFIG [15]

Furthermore, two control modes can be applied to the DFIG, as follows:

Power Factor Control mode – the real and reactive powers of the stator are controlled in order to maintain a constant voltage at the point of connection with the grid. Accordingly, in the load flow studies, the DFIG is modelled as a PQ-bus [4].

Voltage Control mode – the voltage is kept constant at the point of common coupling. Accordingly, in the load flow studies, the DFIG is modelled as a PV-bus [18].

In this work, the DFIG is modelled as a PV-bus, for the static voltage analysis, because of its ability to maintain a constant voltage at the point of connection to the utility.

3. Voltage Stability Analysis Techniques

Load flow is used to compute voltage magnitudes and phase angles at all buses. Hence, techniques such as V – P curves, V – Q Sensitivity Analysis, Q – V modal analysis, Q – V curves and minimum singular value method may be applied for voltage stability studies. Voltage stability analysis can be classified as static and dynamic analyses. In the static analysis, 'snapshots' of the system are taken from different time instances in the time domain trajectory, hence, useful information such as voltage stability and proximity to voltage collapse can be derived. Static techniques are sufficient to analyze the voltage stability of a

system. In the dynamic one, a series of first order differential equations are derived and can be solved using any integration method such as Euler Method, Runge-Kutta Methods, numerical stability of explicit integration methods or the implicit integration method [19, 20]. In dynamic analysis, the sequence of events that leads to voltage instability can be analyzed. A complete study period would include the action of equipment with slow dynamics such as tap changers. Only the techniques used in this work are summarized below.

3.1. V – P curves Analysis

The V – P curve at a bus shows the voltage variation versus the real power. The nose point corresponds to the point of voltage collapse (PoVC), or the Saddle-node bifurcation point. The margin between the actual operating point and the PoVC corresponds to the voltage stability margin. Continuation power flow algorithms can be used to obtain the V – P curves.

3.2. Bifurcation Analysis

Both qualitative and quantitative information about the behavior of nonlinear systems close to their 'critical' or bifurcation equilibrium point after variations of the system parameters can be analyzed using the bifurcation theory. In power systems, at least two types of bifurcation have to be discussed [18]:

- Saddle-node Bifurcation (SNB): This type of local bifurcation occurs as two equilibrium points, normally one unstable and one stable, merge and disappear. Mathematically, this corresponds to the singularity of the Jacobian matrix. In the V – P curve, this will correspond to the nose point.
- Hopf Bifurcation (HB): This occurs as a result of two conjugate pair of eigenvalues becoming pure imaginary. Consequently, more oscillatory becomes the system, hence, stability may be lost by increasing the amplitude of the oscillation [18].

3.3. Q – V Modal Analysis

Voltage is strongly related to the reactive power. Real power may be kept constant at each operating point and voltage stability may be evaluated using the incremental relationship between *Q* and *V*. The reduced Jacobian matrix (J_R), derived from the Jacobian matrix, can be expressed as follows:

$$\Delta Q = J_R \Delta V \tag{7}$$

In addition, J_R can be factored as follows:

$$J_R = x\Lambda^{-1}\eta \tag{8}$$

where: (x) is the right eigenvector matrix of J_R, (Λ) is the diagonal eigenvector matrix of J_R and (η) is the left eigenvector matrix of J_R. Equations (9) and (10) show the voltage variation with the reactive power.

$$\Delta V = x\Lambda^{-1}\eta\Delta Q \tag{9}$$

$$\Delta V = \sum_i \frac{x_i \eta_i}{\lambda_i} \Delta Q \tag{10}$$

where: x_i is the *i*th column of the right eigenvalue of J_R, η_i is the *i*th row of the left eigenvalue of J_R, λ_i is the *i*th eigenvalue of J_R obtained from the diagonal matrix Λ^{-1}. For the *i*th mode, the modal voltage variation is given by (11).

$$v_i = \frac{1}{\lambda_i} q_i \tag{11}$$

Eigenvalues of the reduced Jacobian matrix are used as indicators of voltage stability. If all the eigenvalues are positive, the system is considered voltage stable. On the other hand, the system is considered voltage unstable if at least one of the eigenvalues is negative or equals zero. Accordingly, the smaller the value of positive λ, the closer the system is to voltage instability. However, the magnitude of the eigenvalue may not provide an absolute measure to voltage instability due to the nonlinearity of the power flow problem. Consequentially, the V – Q sensitivity at a bus *k* is given by (12).

$$\frac{\partial V_k}{\partial Q_k} = \sum_i \frac{x_{ki}\eta_{ki}}{\lambda_i} \quad (12)$$

If the V – Q sensitivity is negative, this implies that the system is unstable. Smaller the sensitivity, the more stable is the system. Another quantity which can be derived is the participation factor of the bus *k*. It determines the areas associated with each mode as given in (13). Additionally, the entire bus participation factors for each mode sum up to unity.

$$P_{ki} = x_{ki}\eta_{ki} \quad (13)$$

Generally, there are two modes. In the first one, only few buses have large participation factors and the others will have participation close to zero. In the second mode, many buses have small and similar participation factors, whilst the others have participations close to zero. Mode one occurs if a load is connected to a very strong network. Mode two occurs when a region is heavily loaded with the reactive power reserve exhausted.

3.4. Dynamic Analysis

This involves performing time domain simulations. Power system and its components are usually represented by a set of nonlinear differential algebraic equations. Time integration methods are used to solve equations these nonlinear equations. Methods exist are the Euler method, Runge-Kutta Methods and Trapezoidal Rule. These methods are described in [20].
In this work, trapezoidal rule is used because of its simplicity and robustness. Besides, it is used in many commercial softwares [21]. In this paper, dynamic analysis is used to capture the time-domain response of the STATCOM and the SVC in response to a contingency.

4. FACTS and Placement Methods

By definition, FACTS are alternating current transmission systems consisting of power electronic devices and other static controllers that improve controllability and increase power transfer capability [6]. They can be interfaced with an energy storage element to supply or absorb active and reactive powers. Due to the high speed operation of these controllers; both

steady-state and dynamic conditions can be controlled. In this paper, STATCOM and SVC are used as reactive power compensators, while taking into account maintaining the voltage magnitude within its statutory limits.

The IEEE Working Group on FACTS defines the STATCOM as a static synchronous generator connected in parallel with the load, it can control the reactive power with variable inductive or capacitive current which does not depend on the system voltage [22]. Figure (3) shows the STATCOM and its V – I characteristics. The previous definition of STATCOMs can be fragmented into three components. Firstly, it is 'static' which implies it has no rotational part and is based on solid state switches. Secondly, it is 'synchronous' which is related to three phase synchronous machines. Thirdly, 'compensator' can be seen as providing reactive power support. The STATCOM presents several advantages such as quick time response, small size, good dynamic characteristics under various operating conditions, and accurate voltage control. The voltage source converter (VSC) is the heart of the STATCOM. It consists of a self-commutating solid-state turn off devices such as GTO and IGBT together with a reverse blocking diode in parallel. The switches operate either in the square wave mode, pulse width modulation mode with a high switching frequency or selective harmonic elimination modulation technique. A DC capacitor is connected to the input side of the VSC to provide the required DC input voltage. The output of the VSC is nearly sinusoidal with the use of filters [23] . The main purpose of the STATCOM is to generate sinusoidal waveform at the point of common coupling and control the flow of reactive current. The STATCOM can inherently supply active power as well. It is controlled by the phase angle between the converter output and the AC main voltage. The reactive power is controlled by the voltage magnitude of the converter output voltage and the AC main voltage.

On the other side, the IEEE Working Group on FACTS defines the SVC as a generator that is capable of generating or absorbing reactive power (variable reactive current capability) when connected in parallel with a load, hence the desired parameters such as voltage can be controlled. The SVC and its V – I characteristic are shown in Figure (4). It consists of a thyristor-controlled reactor in an arm with a capacitor in the opposite arm. Varying the phase

angle, a continuous range of reactive power variation can be achieved. The main drawbacks of this setting are the production of low-order harmonics and high losses while working in the inductive region. The FACTS models present in PSAT are described in [24].

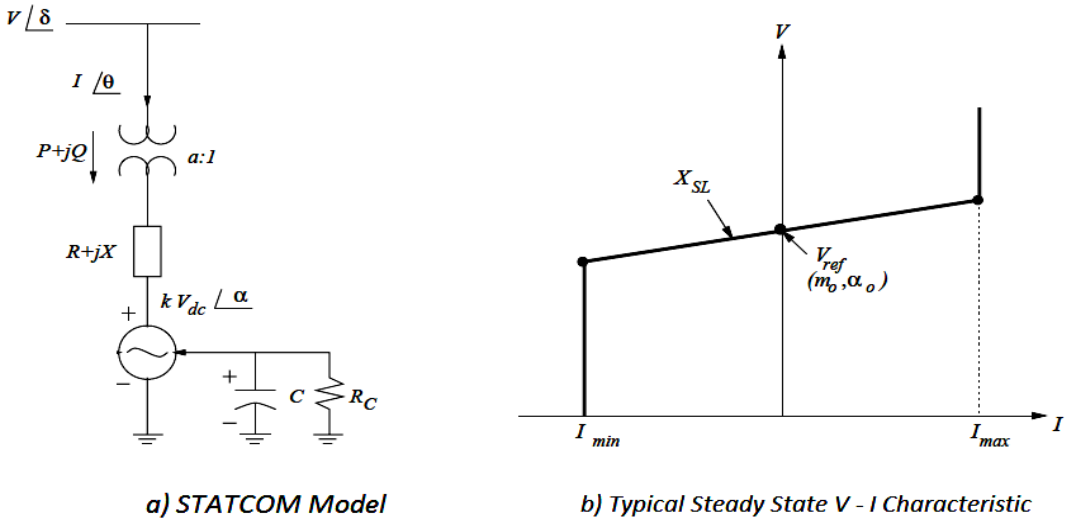

Figure 3. STATCOM model and its corresponding V – I characteristic [21]

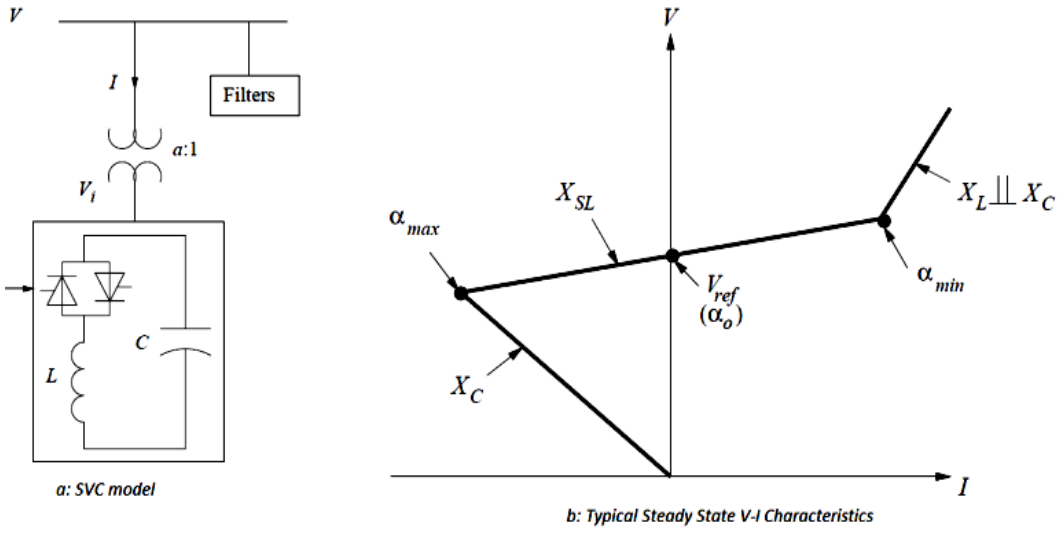

Figure 4. SVC model and its corresponding V – I characteristic [21]

In its broadest scene, FACTS placement techniques can be classified into three main categories [25-27] which are highlighted and described below.

Artificial Intelligence Based Techniques: Artificial Intelligence (AI) is human-made systems

that possess some of the important characteristics of life. The algorithms that have been used are the Genetic Algorithm, Tabu Search Algorithm, Simulated Annealing Algorithms, Particle Swarm Optimization, Ant Colony Optimization, Fuzzy Logic Algorithm, Harmony Search Algorithm and Imperialist Competitive algorithm.

Optimization Based Methods: Non-linear programming, Integer and Mixed-integer programming, and Dynamic programming techniques are all belonging to this category.

Sensitivity Based Methods: Minimum singular value decomposition and eigenvalue analysis, fall into this category. In [28], sensitivity-information such as the rate of change of voltage with reactive power and the rate of change of losses with real and reactive power are derived from the reduced Jacobian matrix. By 2016, this information will be used for Unified Power Flow Controllers (UPFCs) placement in the Iranian network.

5. Formulation of the Search Algorithm

A simple algorithm for the placement of the FACTS devices using static analysis is proposed. Figure (5) demonstrates a flowchart for the placement of these devices, STATCOM and the SVC. Q – V modal analysis is used to check the stability of the system, and the weakest buses are identified using the eigenvalues and the participation factors. The target voltage of the network is set according to the ANSI Standard C84.1 guidelines [29] given in Table 1. For voltage below 46 kV, Range A corresponds to the ideal or optimal voltage limits whereas Range B is acceptable but not desirable. For voltage above 46 kV, the two ranges, namely normal operating and emergency condition, are defined. Consequentially, the power flow is used to find the reactive power requirement so that the STATCOM and SVC can be sized. After compensation, all voltage limits in the network are re-checked. If the compensated voltage violates its permissible values, the above processes are repeated again. The IEEE 14-bus test system is used for case studies. The numerical data were primarily taken from [30]. The test network with its bus labels is shown in Figure (6).

The proposed algorithm is implemented by programming in MatLab and PSAT environments. PSAT can be run through the MatLab interface using command line technique. This enables

solving large systems. On the other side, this method may present some computing and time challenges in a system comprising of thousands of buses. It becomes financially impractical to place a FACTS compensator at each bus to maintain voltage magnitude at its desired level. Generally, to overcome this challenge, a network is divided into different regions called pilot nodes. These pilot nodes represent the voltage in these regions. Hence, the presented flowchart can be applied to maintain voltage within tight tolerances at these nodes.

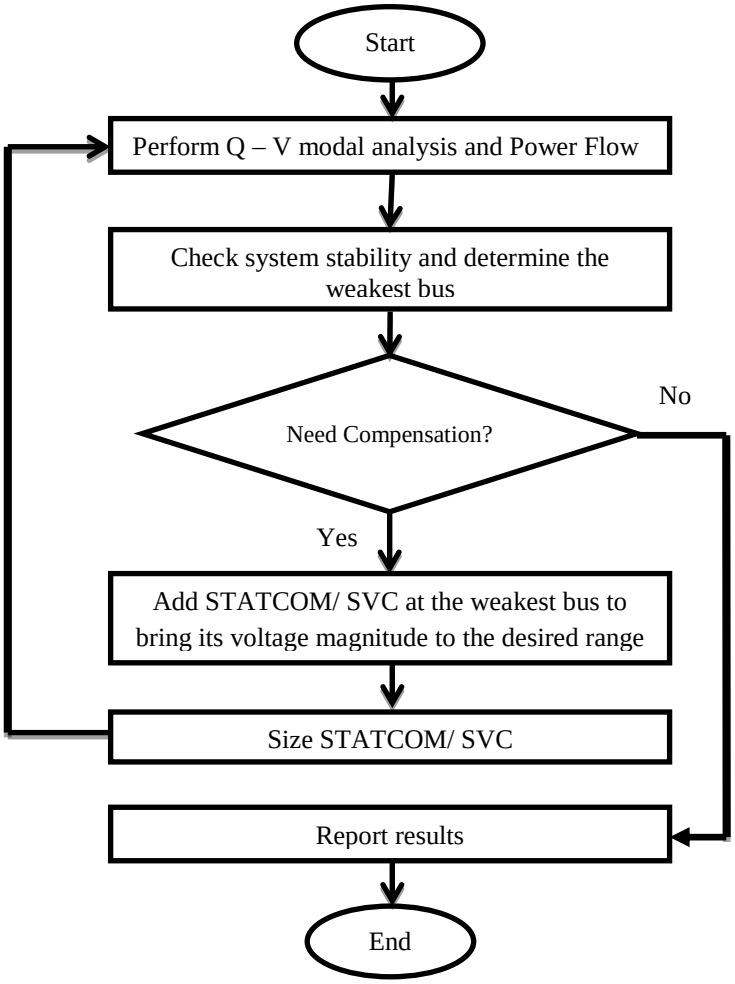

Figure 5. Flowchart for FACTS placement

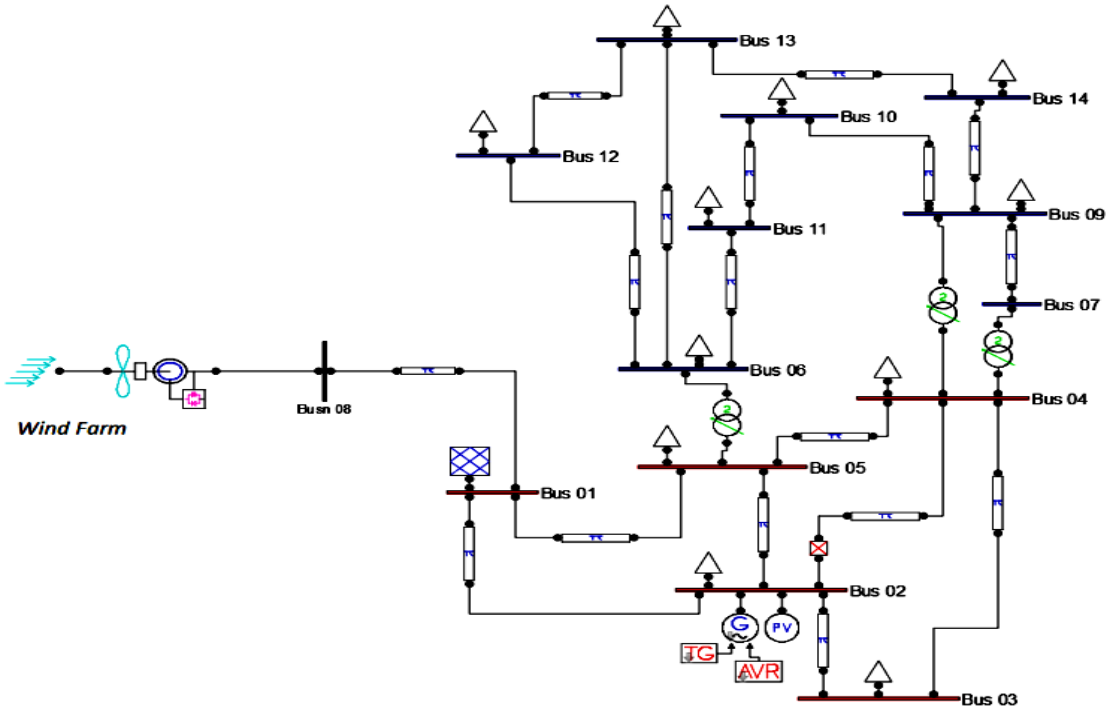

Figure 6. IEEE 14-bus test system [27]

Table 1
Voltage levels, according to ANSI C84.1

Voltage Levels	Range A		Range B	
	Minimum value (pu)	Maximum value (pu)	Minimum value (pu)	Maximum value (pu)
2.4 kV – 35.4 kV	0.975	1.05	0.95	1.058
Above 46 kV	Normal Condition		Emergency Condition	
	Minimum value (pu)	Maximum value (pu)	Minimum value (pu)	Maximum value (pu)
	0.95	1.06	0.90	1.10

6. Simulation Results and Discussion

6.1 Static Analysis

Firstly, simulation results are presented without reactive power compensation and the results are examined in details. The first study performed is solving the power flow using the full Newton-Raphson algorithm, with reactive power limits of the system taken into consideration. The results of the uncompensated system are given in Table 2.

Table 2
Results of the uncompensated load flow

Bus No.	Initial Bus Type	Voltage (pu)	Angle (rad)	P Injection (pu)	Q Injection (pu)
1	Slack	1.0600	0	1.583	1.49
2	PV	1.0103	-0.0809	0.183	0.373
3	PQ	0.9263	-0.2216	-0.942	-0.19
4	PQ	0.9404	-0.1734	-0.478	-0.04
5	PQ	0.9529	-0.1462	-0.076	-0.016
6	PQ	0.9468	-0.2632	-0.112	-0.075
7	-	0.9305	-0.2381	0	0
8	PV	1	0.0780	0.78	-0.645
9	PQ	0.9158	-0.2738	-0.295	-0.166
10	PQ	0.9127	-0.2783	-0.09	-0.058
11	PQ	0.9256	-0.2735	-0.035	-0.018
12	PQ	0.9288	-0.2822	-0.061	-0.016
13	PQ	0.9222	-0.2833	-0.135	-0.058
14	PQ	0.8978	-0.301	-0.149	-0.05

Initially, Bus 2 was set as a PV bus with voltage being 1.045 pu. However, after the load flow, the voltage is 1.0103 pu, because of the bus-switching occurs from PV to PQ, as a result of reactive power limits of the generator at Bus 2 being exceeded. Hence, it can be concluded that there is a lack of reactive power support at the generator of Bus 2. The negative sign of reactive power injection at Bus 8 reflects the ability of the DFIG to absorb reactive power. Additionally, the voltage level is below 0.975 pu, which is the lowest acceptable limit according to the ANSI C84.1. Bus 14 has the lowest voltage followed by bus 10 and bus 13. This occurs as they are far from generation, and suffer from the voltage drop across transformers and transmission lines.

The second study performed was Q–V modal analysis. The results are given in Table 3. All the eigenvalues of the reduced Jacobian matrix are positive with no imaginary part indicating that the system is stable. According to Equation (12), the smaller the value of positive λ, the closer the system is to voltage instability. Thus, the bus having the highest participation factor associated with this eigenvalue is the weakest bus. From Table 3, it can be seen that the smallest eigenvalue is number 5 (0.413), and Bus 14 has the largest participation factor

(0.1388) associated with this eigenvalue. Hence, Bus 14 is the weakest bus.

Table 3
Modal Analysis Results

Eigenvalue No.	Most Associated Bus	Eigenvalue	Participation factor of most associated buses
1	Bus 04	61.035	0.5315
2	Bus 02	37.332	0.8671
3	Bus 09	34.138	0.6392
4	Bus 06	25.564	0.6405
5	Bus 14	0.413	0.1388
6	Bus 05	17.367	0.2664
7	Bus 13	15.853	0.3491
8	Bus 12	13.156	0.2289
9	Bus 12	3.159	0.3199
10	Bus 11	8.789	0.2868
11	Bus 14	5.670	0.4418
12	Bus 03	5.025	0.4059
13	Bus 01	999	1
14	Bus 08	9.291	1

The third study performed was the V–P curve analysis using the Continuation Power Flow. It is used to obtain the voltage profile at each bus with the generation limits taken into consideration. The results for the PV buses are shown in Figure (7) and the results for the buses associated with the lowest eigenvalues are shown in Figure (8). The maximum loading parameter $\lambda_{critical}$, corresponds to the limit the system can be loaded before voltage instability occurs, is found to be 1.425. It can be observed that Bus 14 has the lowest voltage at the SNB point and ultimately collapsed to zero. At Bus 2, the voltage profile is not constant as the generator is already operating at its upper reactive limit.

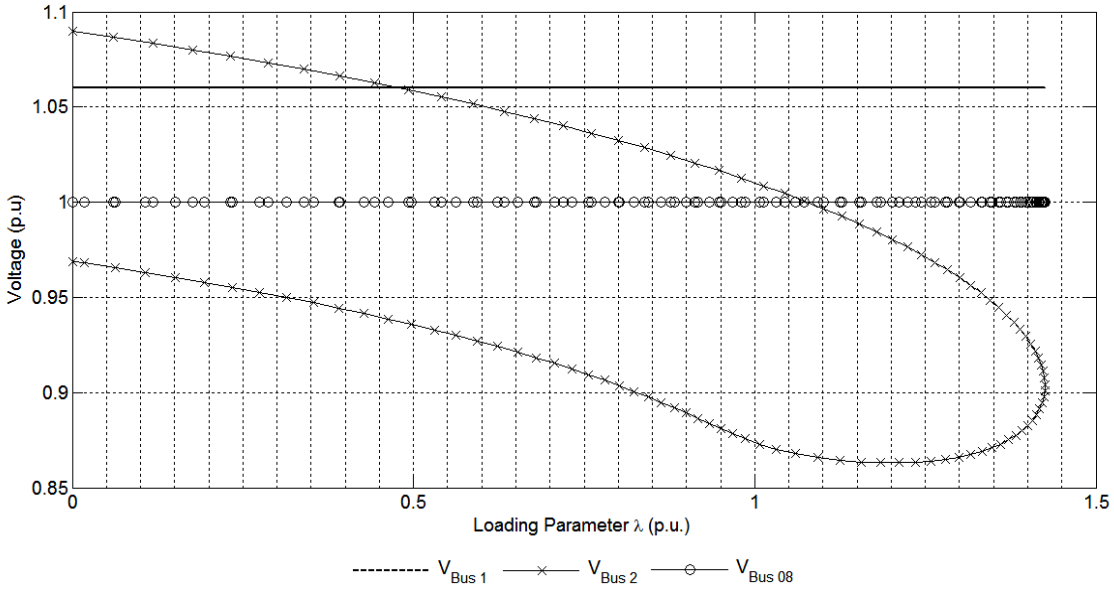

Figure 7. V - P Curves for the PV Buses

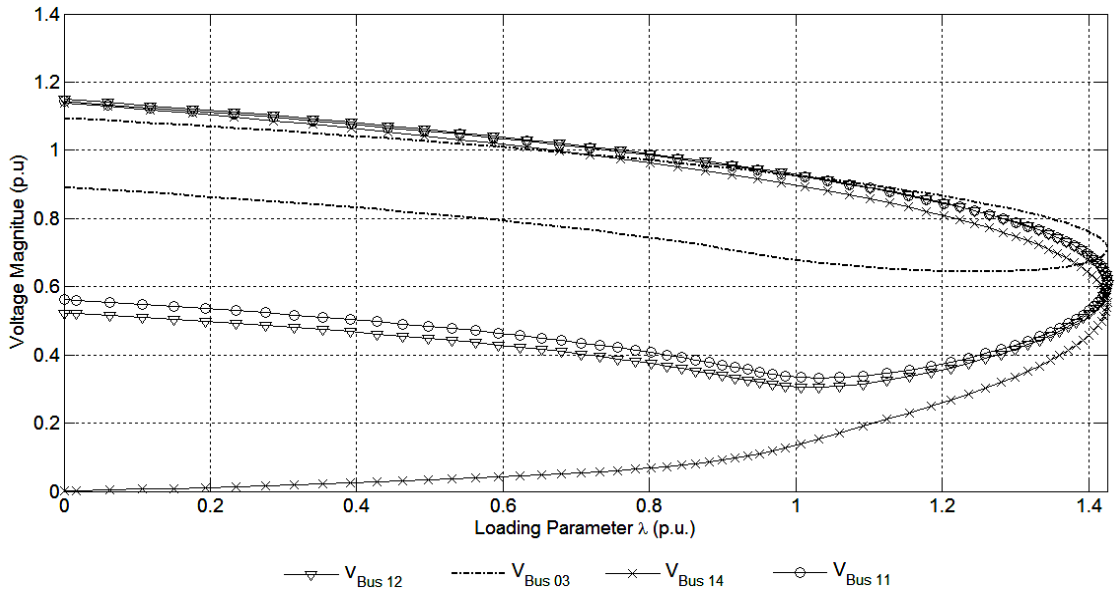

Figure 8. V - P Curves for PQ Buses having worst eigenvalues

Moreover, Figure (9) shows the different voltage magnitudes at the Saddle Node Bifurcation point. This represents the lowest voltage at each bus before voltage collapse. Once more, it can be seen that Bus 14 has the lowest voltage magnitude.

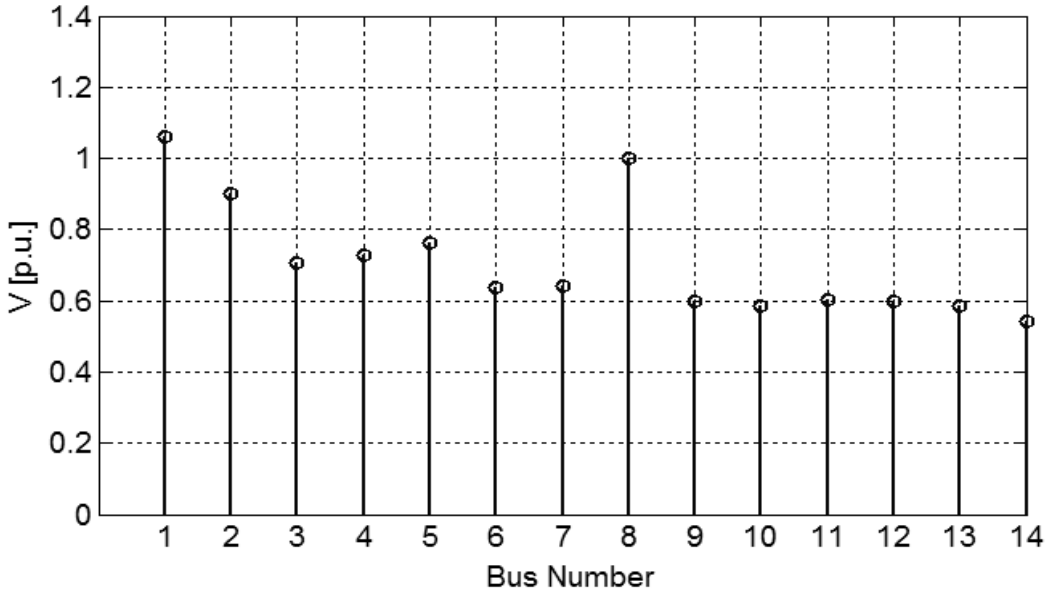

Figure 9. Voltage Magnitudes Profile at the Bifurcation Point

The reactive power required to bring the voltage within limits is calculated using the flowchart shown in Figure (5). Two iterations are required to bring the voltage within limits. The first iteration places a compensator at Bus 14. The system is re-checked for voltage stability. Consequentially, the second iteration places a compensator at Bus 03. Re-checking the system for voltage stability, the target voltage has been achieved with the two compensators. The voltage magnitudes at each iteration are given in Table 4. Consequentially, the power flow results after compensation is shown in Table 5.

Table 4
Voltage Magnitude at each iteration

Bus No.	Voltage Magnitude (pu)	
	1st Iteration	2nd Iteration
1	1.06	1.06
2	1.0224	1.0363
3	0.9481	1.0
4	0.9680	0.9888
5	0.9781	0.9944
6	1.004	1.0154
7	0.9802	0.9957
8	1.0	1.0
9	0.9766	0.9891
10	0.9734	0.9858
11	0.9846	0.9967
12	0.9919	1.0024
13	0.9901	0.9994
14	1.0	1.0

Table 5
Power Flow results after compensation

Bus No.	Voltage (pu)	Angle (rad)	P Injection (pu)	Q Injection (pu)	Q Generation (pu)
1	1.06	0	1.561	0.847	0.847
2	1.0363	-0.0858	0.183	0.373	0.5
3	1.0	-0.2254	-0.942	0.159	0.349
4	0.9888	-0.1760	-0.478	-0.04	-
5	0.9944	-0.1494	-0.076	-0.016	-
6	1.0154	-0.2536	-0.112	-0.075	-
7	0.9957	-0.2335	0	0	-
8	1.0	0.0798	0.78	-0.645	-0.645
9	0.9891	-0.2644	-0.295	-0.166	-
10	0.9858	-0.2680	-0.09	-0.058	-
11	0.9967	-0.2632	-0.035	-0.018	-
12	1.0024	-0.2711	-0.061	-0.016	-
13	0.9994	-0.2746	-0.135	-0.058	-
14	1.0	-0.3002	-0.149	0.117	0.167

The V – P curve analysis is used to check the new loadability limit of the system using the CPF, without any voltage limits. The new critical loading parameter is 2.756. This represents an increase of 93.4%, without reactive power limits enforced, which is calculated using Equation (14). Hence, providing reactive power compensation will increase the loadability of the system. This is particularly important where system operator wants to defer investment in assets, but want to increase capacity of transmission lines The V – P curves for the PQ buses are shown in Figures (10) and (11), respectively.

$$\%\ \text{Increasing in Loading} = \frac{\lambda_{critical}\left(\text{with compensation}\right) - \lambda_{critical}\left(\text{without compensation}\right)}{\lambda_{critical}\left(\text{without compensation}\right)} \times 100 \quad (14)$$

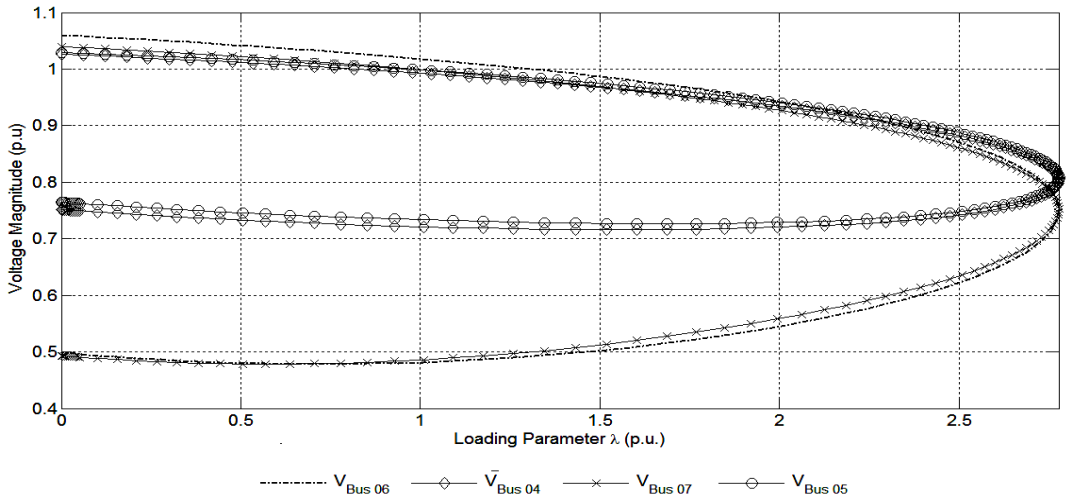

Figure 10. V - P Curves for compensation for Buses 4 to 7

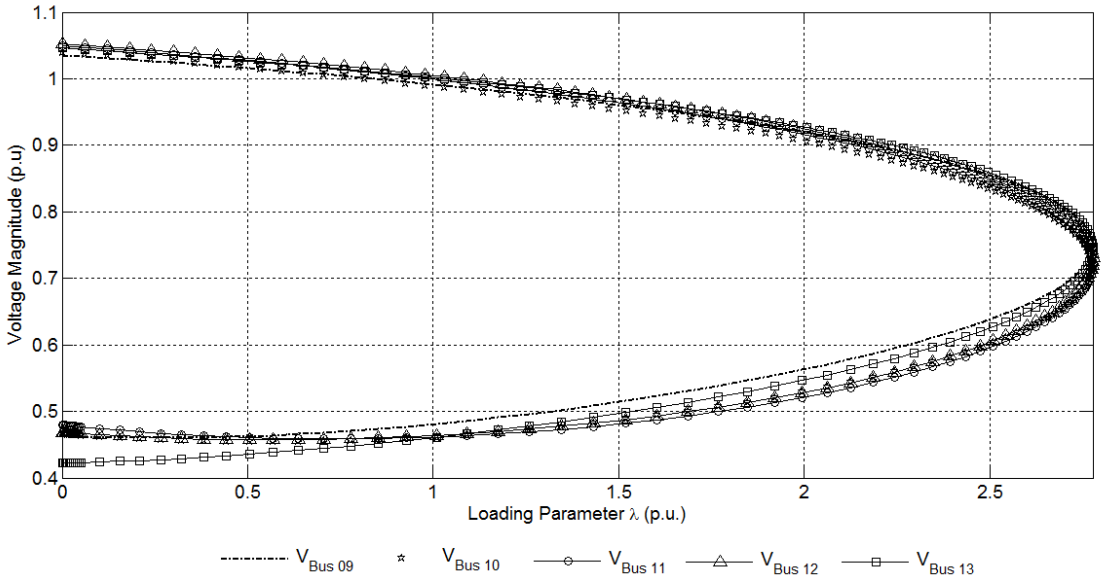

Figure 11. V – P curves after compensation for Buses 9 to 13

The load flow results give basic data required to specify the normal operating condition of the compensators. However, during the planning, the level to which the system will be stretched must be taken into consideration. CPF can be used to find the loading parameter that causes the voltage magnitude of a PQ bus to reach the acceptable and emergency rating of the ANSI C84.1. The result is depicted in Table 6. It can be observed that during normal operation, the system can be loaded up to 1.382 before Bus 11 attains the 0.975 pu of the ANSI C84.1. Similarly Bus 11 is the first bus to attend the voltage limits in case of the contingency operating condition.

Table 6
Buses attaining their voltage limits with variations of load parameters

Acceptable Operating Limit		Contingency Operating Limit	
Load Parameter, λ	Bus number attaining its voltage limit	Load parameter, λ	Bus number attaining its voltage limit
1.382	11	1.722	11
1.417	13	1.757	13
1.451	12	1.791	12
1.486	10	1.825	10
1.521	9	1.860	9
1.893	5	1.894	6
1.927	6	2.515	5
1.962	4	2.534	4

When this loadability limit is reached, a load flow is performed again to obtain the reactive power limit of the compensators. Their specifications are given in Table 7. Additionally, for the compensated system, the real power loss decreases by 12.7% and the reactive power loss decreases by 23.7%. The huge decrease of the reactive power loss is that it is being supplied locally at Bus 14 and Bus 03. Hence, it does not have to be transmitted via power lines and thus no losses.

Table 7
Compensators specifications

	Q (Mvar)		V (kV)	f (Hz)
	Nominal Rating	Emergency Rating		
Compensator at Bus 14	16.7	59.0	13.8	60
Compensator at Bus 03	34.9	103.6	69.0	60

6.2 Dynamic Analysis (Time Domain) Response of FACTS

Other parameters that need to be specified are the desired switching technology and permissible active power losses. The response time and type of response (maximum overshoot and settling time) determines the time required by the compensators to bring voltage to its pre-disturbed condition, or to a new stable operating point. These can be obtained by performing a dynamic simulation. Consequentially, dynamic analysis is used to observe the response of the STATCOM and the SVC under normal and contingency conditions.

The response of the FACTS devices at Bus 03 is observed. Loss of line 2-3 is simulated at a time (t) equals 20 seconds. Their performance is analyzed and their limits have not been exceeded.

The STATCOM and SVC responses are compared, as shown in Figure (12). It can be observed that both the STATCOM and the SCV are able to bring the voltage at the considered buses to 1 pu when neither the STATCOM nor the SVC has attained their limits. Hence, it can be concluded that both compensators have the same voltage support capability when they

are operating within their limits. This corresponds to the linear region of the V – I characteristic of theses devices.

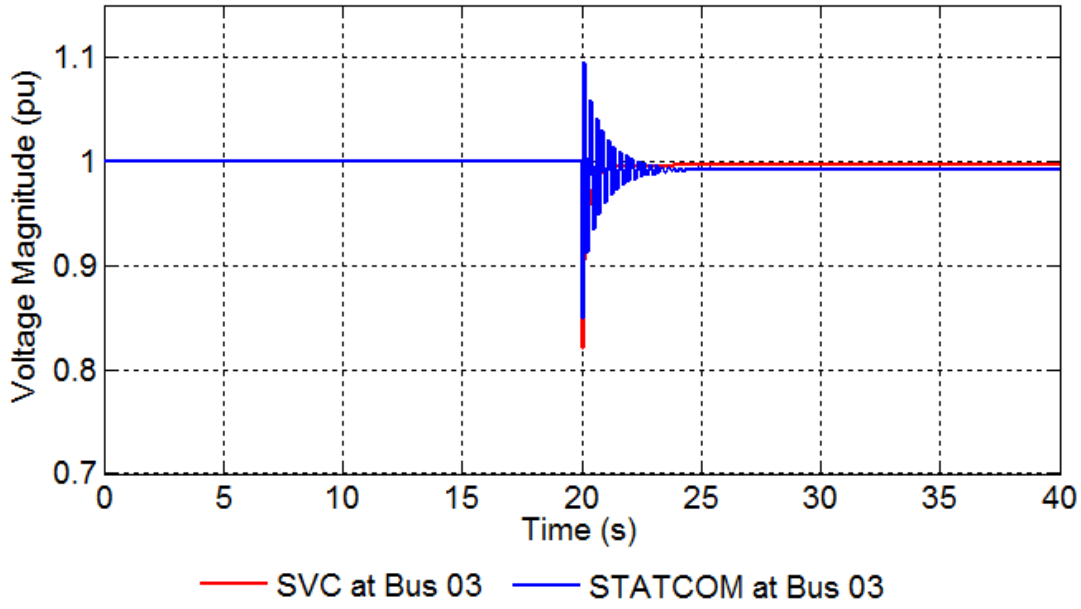

Figure 12. Response time of the SVC and the STATCOM at Bus 3

Furthermore, the simulation is re-performed with the STATCOM and the SVC operating at their lowest reactive power limit. The voltage profile at bus 03 is analyzed again, as shown in Figure (13).

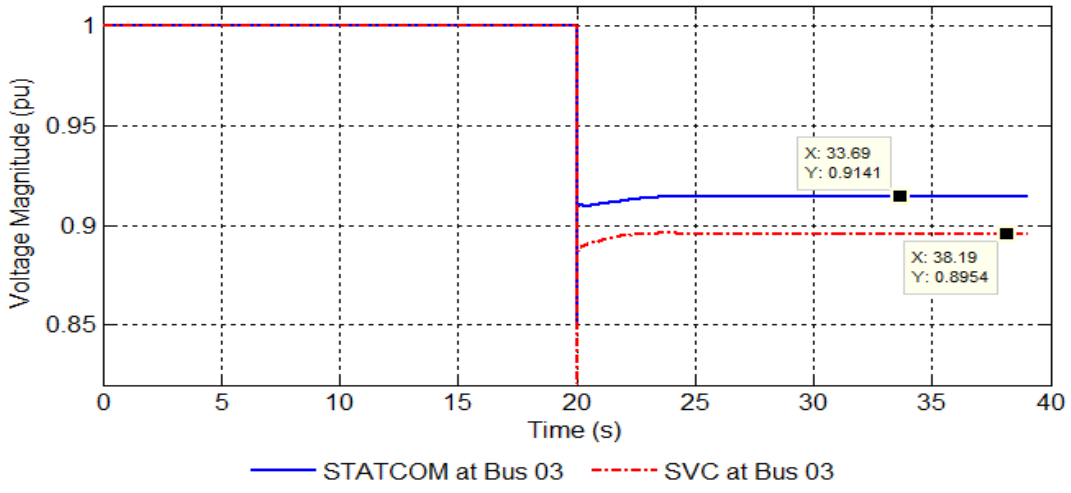

Figure 13. Bus 03 with FACTS compensators having reduced reactive power

It can be seen that the STATCOM provides better voltage support at its lower limit compared to the SVC at the same conditions. The steady voltage magnitude after the line outage with STATCOM is 0.914 pu and 0.895 pu with the SVC. When the SVC operates at its low reactive power limit, it behaves as a fixed shunt reactance, and the amount of reactive power it can provide or sink depends on the voltage of its bus. Theoretically, the reactive power output at the limits is proportional to the square of this voltage. On the other hand, the STATCOM is a current limited device. It can provide a constant reactive current at its limit. Hence, the STATCOM is more useful in preventing voltage collapse than the SVC.

7. Conclusions

For proper operation of the grid and power system equipment, maintaining voltage stable in a network is crucial. Voltage instability, if not rectified in time, can trigger cascaded events, leading to blackout which can leave the power system in the darks for days. This paper gives an overview of voltage stability phenomenon with wind farm followed by techniques to analyze it. It has been shown that a combination of voltage stability techniques, namely V – P curve, modal and bifurcation analysis can be used to study voltage stability of a network. A solution to increase stability of the system is to use reactive power controllers. Moreover, it has been shown that STATCOM has superior performance than SVC during contingencies.

References

[1] M. Rozlan, *et al.*, "The Optimisation of Stand-Alone Hybrid Renewable Energy Systems Using HOMER," *International Review of Electrical Engineering*, vol. 6, 2011.

[2] T. R. Ayodele, *et al.*, "Challenges of Grid Integration of Wind Power on Power System Grid Integrity: A Review," *International Journal of Renewable Energy Research (IJRER)*, vol. 2, pp. 618-626, 2012.

[3] P. Kundur, *et al.*, "Definition and classification of power system stability IEEE/CIGRE joint task force on stability terms and definitions," *Power Systems, IEEE Transactions on*, vol. 19, pp. 1387-1401, 2004.

[4] M. Guleryuz and A. Demiroren, "Effects of a wind farm and FACTS devices on static voltage stability of Bursa transmission system in Turkey," in *Environment and Electrical Engineering (EEEIC), 2011 10th International Conference on*, 2011, pp. 1-5.

[5] C. Angeles-Camacho, *et al.*, "FACTS: its role in the connection of wind power to power networks," in *Modern Electric Power Systems (MEPS), 2010 Proceedings of the International Symposium*, 2010, pp. 1-7.

[6] N. G. Hingorani, "FACTS Technology - State of the Art, Current Challenges and the Future Prospects," in *Power Engineering Society General Meeting, 2007. IEEE*, 2007, pp. 1-4.

[7] H. Tarafdar, *et al.*, "Dynamic stability improvement of a wind farm connected to grid using STATCOM," in *Electrical Engineering/Electronics, Computer, Telecommunications and Information Technology, 2008. ECTI-CON 2008. 5th International Conference on*, 2008, pp. 1057-1060.

[8] M. I. Marei and H. S. El-Goharey, "Dynamic performance analysis of a wind farm equipped with STATCOM," in *Power Engineering, Energy and Electrical Drives (POWERENG), 2013 Fourth International Conference on*, 2013, pp. 421-426.

[9] B. Maya, *et al.*, "An integrated approach for the voltage stability enhancement of large wind integrated power systems," in *Power, Signals, Controls and Computation (EPSCICON), 2012 International Conference on*, 2012, pp. 1-6.

[10] V. Salehi, *et al.*, "Improvement of voltage stability in wind farm connection to distribution network using FACTS devices," in *IEEE Industrial Electronics, IECON 2006-32nd Annual Conference on*, 2006, pp. 4242-4247.

[11] R. Natesan and G. Radman, "Effects of STATCOM, SSSC and UPFC on Voltage Stability," in *System Theory, 2004. Proceedings of the Thirty-Sixth Southeastern Symposium on*, 2004, pp. 546-550.

[12] B. Cui, *et al.*, "Analysis on the static voltage stability of an actual power system with large-scale wind farm," in *Renewable Power Generation Conference (RPG 2013), 2nd IET*, 2013, pp. 1-5.

[13] R. Fu, *et al.*, "Study on application of STATCOM in voltage stability of wind farm incorporated system," in *Control Conference (CCC), 2013 32nd Chinese*, 2013, pp. 8868-8873.

[14] E. H. Camm, *et al.*, "Characteristics of wind turbine generators for wind power plants," in *Power & Energy Society General Meeting, 2009. PES '09. IEEE*, 2009, pp. 1-5.

[15] Y. Zhang and S. Ula, "Comparison and evaluation of three main types of wind turbines," in *Transmission and Distribution Conference and Exposition, 2008. T&# x00026; D. IEEE/PES*, 2008, pp. 1-6.

[16] S. Simani, *et al.*, "Wind turbine simulator fault diagnosis via fuzzy modelling and identification techniques," *Sustainable Energy, Grids and Networks*, vol. 1, pp. 45-52, 2015.

[17] L. Yazhou, *et al.*, "Modeling of the wind turbine with a doubly fed induction generator for grid integration studies," *Energy Conversion, IEEE Transactions on*, vol. 21, pp. 257-264, 2006.

[18] Z. Zhiyuan, *et al.*, "Investigation of Wind Farm on Power System Voltage Stability Based on Bifurcation Theory," in *Power and Energy Engineering Conference, 2009. APPEEC 2009. Asia-Pacific*, 2009, pp. 1-4.

[19] V. Ajjarapu, *Computational techniques for voltage stability assessment and control*: Springer, 2007.

[20] P. Kundur, *et al.*, *Power system stability and control* vol. 7: McGraw-hill New York, 1994.

[21] F. Milano, "An open source power system analysis toolbox," *Power Systems, IEEE Transactions on*, vol. 20, pp. 1199-1206, 2005.

[22] N. G. Hingorani, *et al.*, *Understanding FACTS: concepts and technology of flexible AC transmission systems* vol. 1: IEEE press New York, 2000.

[23] A. M. Saeed, *et al.*, "Power conditioning using dynamic voltage restorers under different voltage sag types," *Journal of Advanced Research*, 2015.

[24] C. Cañizares, *et al.*, "Modeling and implementation of TCR and VSI based FACTS controllers," *AT-UCR*, vol. 99, p. 595, 1999.

[25] W. Zhang, *et al.*, "Optimal allocation of shunt dynamic Var source SVC and STATCOM: A Survey," 2006.

[26] H. Ng, *et al.*, "Classification of capacitor allocation techniques," *Power Delivery, IEEE Transactions on*, vol. 15, pp. 387-392, 2000.

[27] R. Bansal, "Optimization methods for electric power systems: An overview," *International Journal of Emerging Electric Power Systems*, vol. 2, 2005.

[28] B. Asadzadeh, *et al.*, "Allocation of UPFC in north west grid of iran to increase power system security," in *Transmission and Distribution Conference and Exposition, 2010 IEEE PES*, 2010, pp. 1-8.

[29] PacifiCorp. 1B.3− Planning Standards for Transmission Voltage [Online]. Available: https://www.pacificpower.net

[30] S. K. M. Kodsi and C. A. Cañizares. Modeling and simulation of IEEE 14 bus system with Facts controllers, Tech. Rep. [Online]. Available: http://www.power.uwaterloo.ca.,